



Ca(II), Zn(II) and Au(III) Sulfamethoxazole Sulfa-drug Complexes: Synthesis, Spectroscopic and Anticancer Evaluation Studies

FATIMA A.I. AL-KHODIR^{1,2}

¹Department of Chemistry, College of Science, Princess Nora Bint Abdul Rahman University, India.

²Deanship of Scientific Research, Princess Nora Bint Adul Rahman University, India.

*Corresponding author E-mail: fatimaalkhodir@yahoo.com

<http://dx.doi.org/10.13005/ojc/310440>

(Received: July 30, 2015; Accepted: September 23, 2015)

ABSTRACT

Herein in this article, three new Ca(II), Zn(II) and Au(III) complexes of sulfamethoxazole (SZ) (sulfa-drug) have been synthesized for the first time. The sulfa-drugs have a great attentions because of their therapeutic applications against bacterial infections. The SZ complexes were discussed with the help of elemental analyses, molar conductance and spectroscopic instruments e.g. IR, ¹H-NMR, and electronic spectra. Investigations of the infrared spectra of the SZ and their metal complexes indicated the vibrations due to the sulfonamido (SO₂ and –NH) and isoxazole (C=N) groups are shifted with respect to the free molecule in line with their coordination to the metal. In case of calcium(II) an zinc(II) complexes, the coordination site of SZ are the sulfonyl oxygen and SO₂-NH sulfonamide nitrogen, but in gold(III) complex, the gold metal ions coordinates through the sulfonyl oxygen and isoxazole nitrogen. These complexes are formulated as: [Ca(SZ)(Cl)₂].8H₂O (1), [Zn(SZ)(Cl)₂].2H₂O (2) and [Au(SZ)(Cl)₂].Cl (3). The molar conductance data reveals that both Ca(II) and Zn(II) complexes are non-electrolyte but gold(III) complex is electrolyte. The morphological nano structures of SZ complexes were checked using X-ray powder diffraction (XRD), scanning electron microscope (SEM) and transmission electron microscopy (TEM). The gold(III) complex was recorded good anticancer behavior against Human colon carcinoma (HCT-116) cells and human hepatocellular carcinoma (HepG-2) cells.

Key words: Sulf-drug, sulfamethoxazole, coordination, nano-size, spectroscopic, anticancer.

INTRODUCTION

Metal–organic frameworks were the interesting field in the last two decades, not only for the physical applications in the areas such as catalysis, molecular adsorption, magnetism,

nonlinear optics, and molecular sensing, but also from their novel topologies and intriguing structural diversities¹⁻³. On the other hand, many organic drugs, which possess modified pharmacological and toxicological properties administered in the form of metallic complexes⁴, have the potential to

act as ligands and the resulting metal–drug complexes are particularly important both in coordination chemistry and biochemistry [5-8], however, the study of metal–drug complexes is still in its early stages, thus representing a great challenge in current synthetic chemistry, coordination chemistry and medicinal bioinorganic chemistry⁹⁻¹¹. Sulfa drugs have attracted special attention for their therapeutic importance as they were used against a wide spectrum of bacterial ailments¹²⁻¹⁴. Also, some sulfa drugs were used in the treatment of cancer, malaria, leprosy and tuberculosis¹⁴.

Sulfamethoxazole (Fig. 1) is a sulfonamide bacteriostatic antibiotic. It is most often used as part of a synergistic combination with trimethoprim in a 5:1 ratio in co-trimoxazole, also known under trade names such as Bactrim, Septrin, or Septra. Its primary activity is against susceptible forms of *Streptococcus*, *Staphylococcus aureus*, *Escherichia coli*, *Haemophilus influenzae*, and oral anaerobes. It is commonly used to treat urinary tract infections. In addition it can be used as an alternative to amoxicillin-based antibiotics to treat sinusitis. It can also be used to treat toxoplasmosis¹⁵.

In literature survey, many authors have been reported the antimicrobial activity of sulfa-drugs and their metal complexes [16-20]. The metal sulfa-drugs chelates have a great pharmacological and physiological rather than their free drugs itself [19, 20]. In this article, the coordination mode of sulfamethoxazole chelating via Ca(II), Zn(II) and Au(III) metal ions have been investigated. The anticancer activities of gold(III) complex were also evaluated upon its nanometric behavior.

EXPERIMENTAL

Chemicals

Sulfamethoxazole (SZ) antibiotic drug was received from the Aldrich chemical company. All of chemicals used in this study were of analytically reagent grade, commercially available from BDH and used without previous purification like CaCl_2 , ZnCl_2 and sodium tetrachloroaurate(III) dehydrate ($\text{NaAuCl}_4 \cdot 2\text{H}_2\text{O}$).

Synthesis

The Ca(II), Zn(II) and Au(II) SZ complexes were prepared similarly according to the following procedure: 1.0 mmol of SZ ligand was dissolved in 25 mL methanol then mixed with 25 mL of methanolic solution of 1.0 mmol of each metal ions (CaCl_2 , ZnCl_2 and $\text{NaAuCl}_4 \cdot 2\text{H}_2\text{O}$). A mixture of 1:1 ratio (metal ions: SZ) was heated under reflux and continuous stirring at 60–70 °C for about 3 h. The mixtures were left overnight until precipitation occurred. The precipitates obtained were filtered off and washed by methanol then left over anhydrous calcium chloride. The yield percent of the products collected were about 70–80%.

Instruments

Carbon, hydrogen and nitrogen analyses have been carried out in Vario EL Fab. CHNS. The amount of water and the metal content percentage were determined by gravimetric analysis method. Infrared spectra of the SZ complexes were recorded on Bruker infrared spectrophotometer in the range of 400-4000 cm^{-1} . The molar conductances of 10^{-3} M solutions of the complexes in DMSO solvent were measured on a HACH conductivity meter model. All the measurements were taken at room temperature for freshly prepared solutions. The electronic spectrum of the complexes were measured in DMSO solvent with concentration of 1×10^{-3} M, in rang 200-800 nm by using Unicam UV/Vis spectrometer. The effective magnetic moment (μ_{eff}) of complexes was measured at room temperature using Gouy's method by a magnetic susceptibility balance from Johnson Metthey and Sherwood model. ¹H-NMR spectra were recorded as DMSO solutions on a Bruker 600 MHz spectrometer using TMS as the internal standard. Thermogravimetric analysis (TGA) experiments were conducted using Shimadzu TGA-50H thermal analyzers. All experiments were performed using a single loose top loading platinum sample pan under nitrogen atmosphere at a flow rate of 30 mL/min and a 10 °C/min heating rate for the temperature range 25-800 °C. SEM images were obtained using a Jeol Jem-1200 EX II Electron microscope at an acceleration voltage of 25 kV. X-ray diffraction (XRD) patterns of the samples were recorded on X Pert Philips X-ray diffractometer. All the diffraction patterns were obtained by using $\text{CuK}_{\alpha 1}$ radiation, with a graphite monochromator at 0.02 °/min scanning rate.

Anti-cancer activities

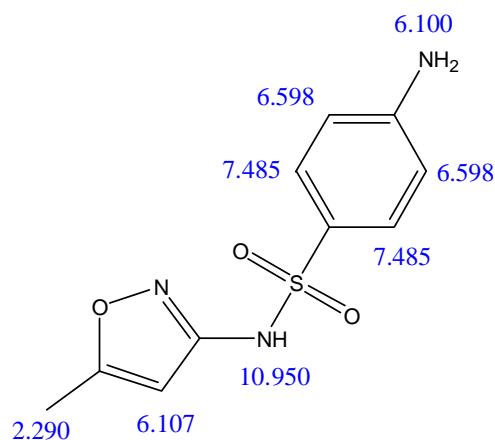
Human colon carcinoma (HCT-116) cells and human hepatocellular carcinoma (HepG-2) cells were obtained from the American type culture collection ATCC, Rockvill, MD). The cells were grown on RPMI-1640 medium supplemented with 10 % inactivated fetal calf serum and 50 µg/mL gentamycin. The cells were maintained at 37 °C in a humidified atmosphere with 5 % CO₂ and were subculture two to three times a week. The cells were grown as monolayers in growth RPMI-1640 medium supplemented with 10% inactivated fetal calf serum and 50 µg/mL gentamycin. The monolayers of 10000 cells adhered at the bottom of the wells in a 96-well micro titer plate incubated for 24 h at 37 °C in a humidified incubator with 5 % CO₂. The monolayers were then washed with sterile phosphate buffered saline (0.01 M pH 7.2) and simultaneously the cells were treated with 100 µL from different dilutions of the test sample in fresh maintenance medium and incubated at 37 °C. A control of untreated cells was made in the absence of the test sample. Six wells were used for each concentration of the test sample. Every 24 h the observation under the inverted microscope was made. The number of the surviving cells was determined by staining the cells with crystal violet²¹,²² followed by cell lysing using 33% glacial acetic acid and read the absorbance at 490 nm using ELISA reader (Sun Rise, TECAN, Inc, USA) after well mixing. The absorbance values from untreated cells were considered as 100% proliferation. The number of viable cells was determined using ELISA reader as previously mentioned before and the percentage of viability was calculated as $[1 - (OD_t/OD_c)] \times 100\%$ where; OD_t is the mean optical density

of wells treated with the test sample and OD_c is the mean optical density of untreated cells. The 50% inhibitory concentration (IC₅₀), the concentration required to cause toxic effect in 50% of inactivated cells, was estimated from graphic plots.

RESULTS AND DISCUSSION

Analytical and physical data

Stable solid SZ complexes were isolated and assigned based on the elemental analyses, spectroscopic data (infrared, UV-Vis., ¹HNMR), molar conductance, and magnetic susceptibility studies. The general formulas (Fig. 2) of the SZ complexes can be depicted as: [Ca(SZ)(Cl)₂].8H₂O (1), [Zn(SZ)(Cl)₂].2H₂O (2) and [Au(SZ)(Cl)₂].Cl (3), respectively. The analytical data together with some physical properties of the complexes are summarized in (Table 1).



Scheme 1: Proton arrangement and chemical shift (ppm) of SZ drug ligand

Table1: Elemental analyses and physical data of SZ free drug ligand and their metal complexes

Empirical formula	Color	m.p/ °C	Δm (mS)	Elemental analysis, % Found % (Calcd.)			
				C	H	N	M
SZ	White	169	14	47.42	4.38	16.59	-
1	White	>250	12	23.51 (23.63)	5.31 (5.35)	8.19 (8.27)	7.39 (7.88)
2	White	>250	23	28.12 (28.22)	3.49 (3.55)	9.79 (9.87)	15.31 (15.36)
3	Yellowish green	>250	84	21.48 (21.58)	1.87 (1.99)	7.43 (7.55)	35.21 (35.39)

The sulfamethazole ligand behaves as a bidentate ligand and coordinate to the metal ions with different place of chelations (O-SO₂ and -NH) and (O-SO₂ and C=N) groups. The isolated SZ complexes are 1:1 molar ratio. The molar conductance values for the Ca(II) and Zn(II) complexes of SZ in DMSO solvent with concentration 1.00 x10⁻³ M were found to be within

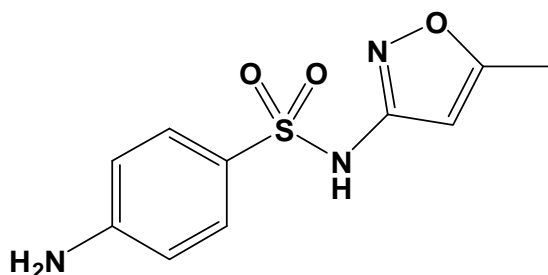


Fig. 1: Sulfamethazole (SZ) drug

the range of 12 and 23 Ω⁻¹.cm².mol⁻¹ at 25 °C, respectively, suggesting them to be non-electrolytes²³, but gold(III) complex has value 84 Ω⁻¹.cm².mol⁻¹ with electrolyte behavior²³. Hence the molar conductance values of Ca(II) and Zn(II) complexes indicate that no ions are present outside the coordination sphere so the Cl⁻ ions exhibit inside the coordination sphere, but the conductance data of gold(III) complex refer that one of chloride ions presence outside of the coordination sphere. The obtained results were strongly matched with the elemental analysis data where Cl⁻ ions are detected after degradation of these complexes by using nitric acid then precipitation of Cl⁻ ions using AgNO₃ reagent.

Infrared spectra

The tentative assignments of the bands for the sulfa-drug ligand (SZ) and their metal complexes

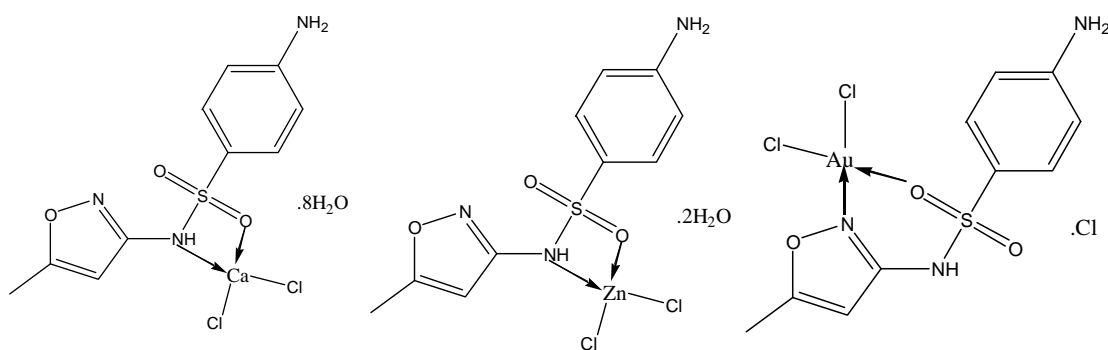


Fig. 2: Suggested formulas of [Ca(SZ)(Cl)₂].8H₂O (1), [Zn(SZ)(Cl)₂].2H₂O (2) and [Au(SZ)(Cl)₂].Cl (3) complexes

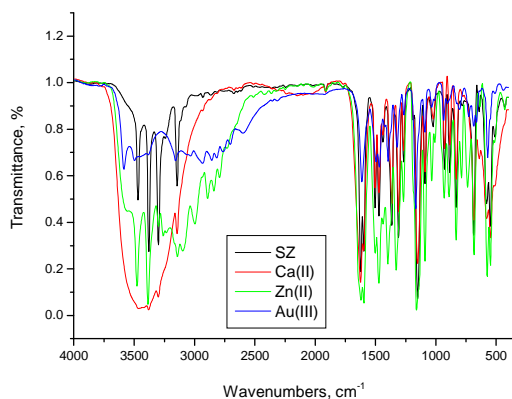


Fig. 3: Infrared spectra of SZ free ligand and their complexes

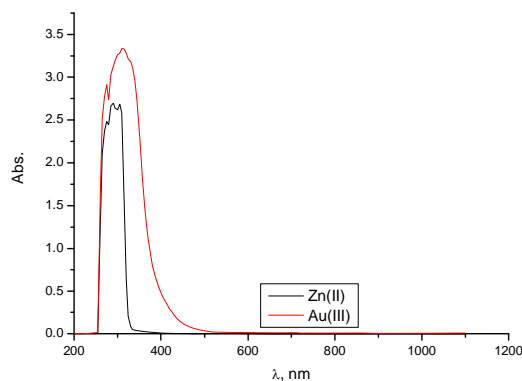


Fig. 4: Electronic spectra of [Zn(SZ)(Cl)₂].2H₂O (2) and [Au(SZ)(Cl)₂].Cl (3) complexes

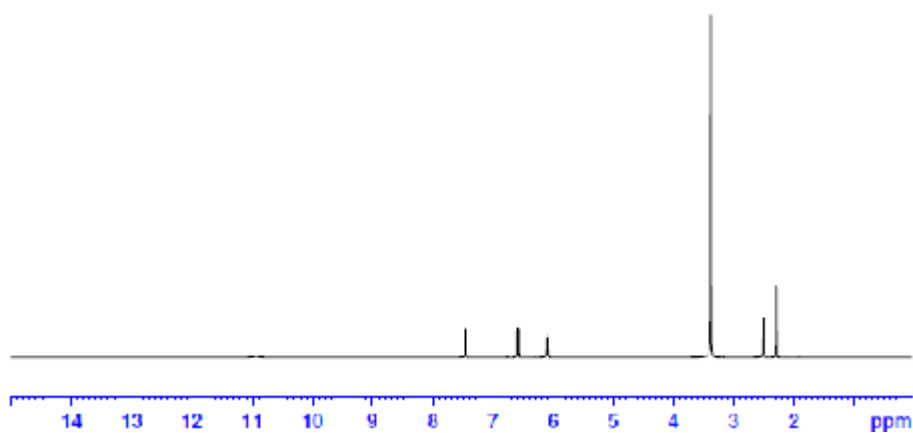


Fig. 5A: ¹H-NMR spectrum of [Ca(SZ)(Cl)₂].8H₂O (1) complex

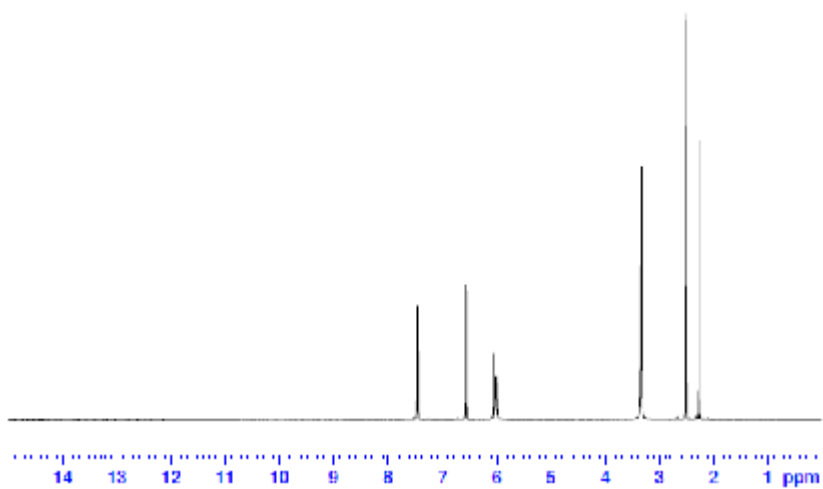


Fig. 5B: ¹H-NMR spectrum of [Zn(SZ)(Cl)₂].2H₂O (2) complex

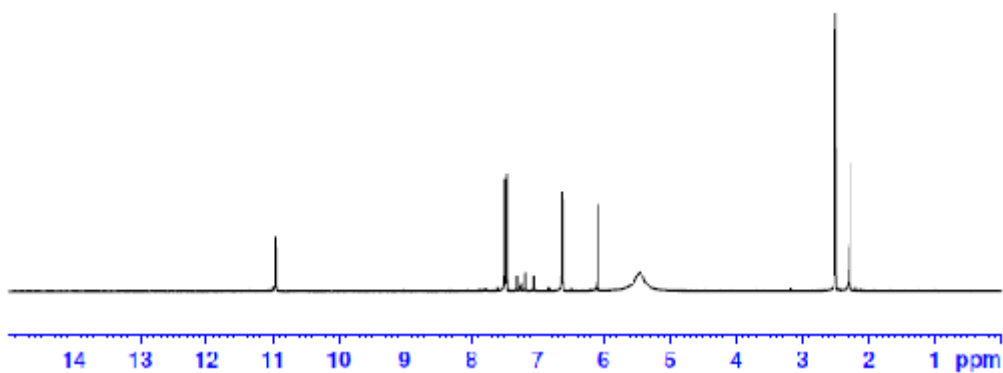


Fig. 5C: ¹H-NMR spectrum of [Au(SZ)(Cl)₂].Cl (3) complex

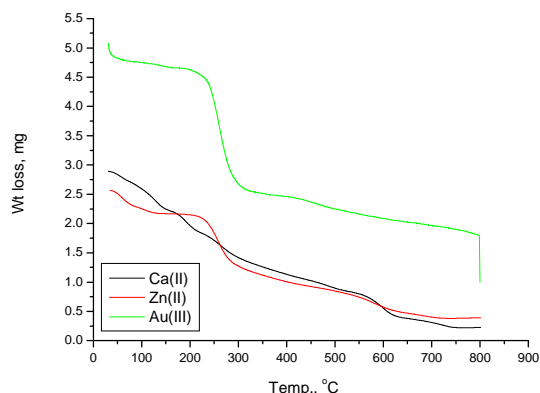


Fig. 6: TGA diagram of Ca(II), Zn(II) and Au(III) SZ complexes

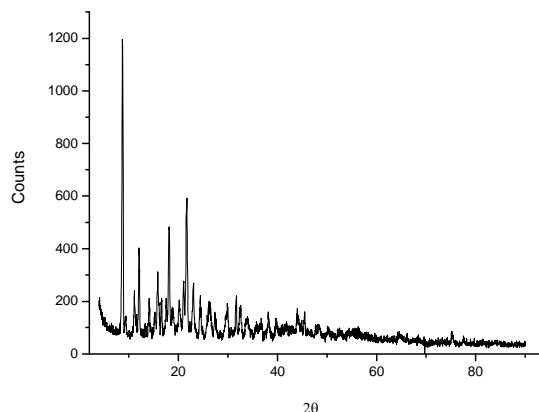


Fig. 7: XRD patterns of [Au(SZ)(Cl)₂].Cl (3) complex

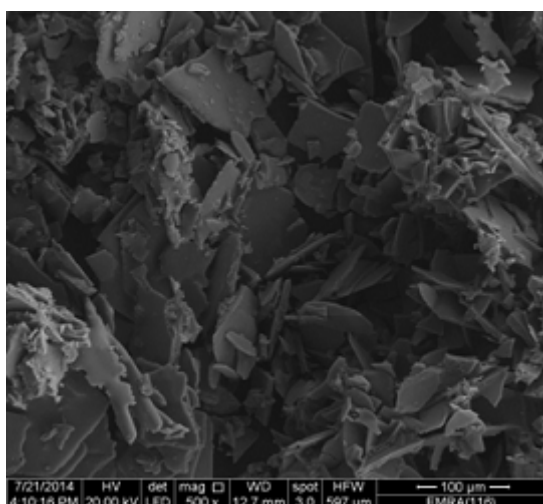


Fig. 8(a): SEM image of [Au(SZ)(Cl)₂].Cl (3) complex

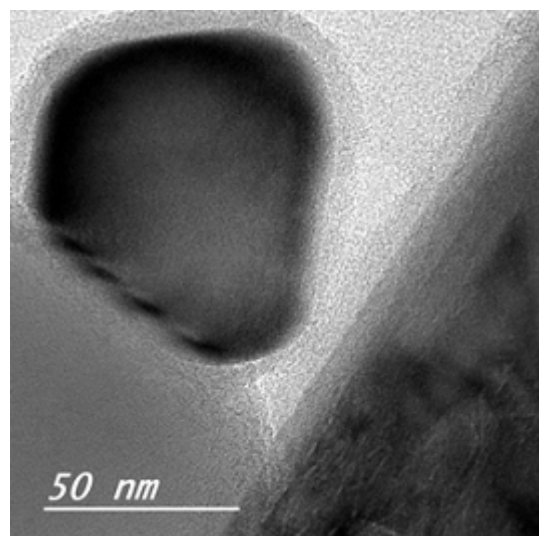


Fig. 8(b): TEM image of [Au(SZ)(Cl)₂].Cl (3) complex

are listed in Table 2 and shown in Fig. 3. The SZ ligand is a potential ligand that can act as a bidentate or tridentate based on its structure so the full infrared assignments are an important technique to identify the chelation mode with different metal ions. Infrared spectrum of the free SZ ligand shows two strong bands at 3468 and 3378 cm^{-1} due to the asymmetric and symmetric stretching vibrations of the $-\text{NH}_2$ amino group²⁴. The medium strong band which appeared at 3299 cm^{-1} is corresponding to the presence of asymmetric sulfonamide $-\text{NH}$ and a very weak band at 3240 cm^{-1} as symmetric frequency. The other band presence at 1623 cm^{-1} is assigned to bending vibration motion of $-\text{NH}_2$ group. The spectrum of SZ has medium bands at

1597 and 1504 cm^{-1} which assigned to the stretching frequency of (C=C) of phenyl ring. The methoxazole ring has three stretching vibration bands at 1472, 1439 and 1365 cm^{-1} . The essential bands exhibited at 1310 and (1188 and 1152) cm^{-1} are due to asymmetric and symmetric stretching frequencies of sulfonyl group^{24, 25}. The bands concerning $-\text{NH}_2$ amino group are unshifted to lower frequencies in case of Ca(II), Zn(II) and Au(III) complexes because of uncoordination toward respected metal ions. The absence of sulfonamide $-\text{NH}$ band in the spectra of the Ca(II) and Zn(II) complexes, indicating the involvement of this group in chelation with central metal ion by nitrogen of this group according to the data reported in literature²⁵. The band related to

isoxazole ring stretching vibrations in free SZ ligand at (1472, 1439 and 1365 cm^{-1}) suffered a shift at (1469 and 1424 cm^{-1}) in the spectra of the gold(III) metal complex indicating that the isoxazole moiety is participation in coordination with gold(III) metal ions [24]. The bands respect to asymmetric and symmetric of sulfonyl group undergoes a shift toward lower or higher frequencies which observed at (1309 and 1152), (1330 and 1161) and (1322 and 1167) cm^{-1} in Ca(II), Zn(II) and Au(III) complexes, respectively. Upon these results, the coordination mode of the SZ ligand with metal ions is a bidentate through the O and N atoms of sulfonylamid group for Ca(II) and Zn(II) complexes except for Au(III) ion coordinated through O and N atoms of sulfonyl and isoxazole. The new bands appeared in the range 400-550 cm^{-1} are due to the stretching frequency of (M-O) and (M-N) bands.

Electronic spectra and magnetic measurements

The UV-Vis. electronic absorption spectrum of the free SZ ligand (Fig. 4) exhibited two absorption bands in the ultraviolet region, the band at 212 nm assigned to the $\pi \rightarrow \pi^*$ transition for the intera-ligand of aromatic system C=C character and a strong absorption band at 270 nm is refer to $n \rightarrow \pi^*$ transition for oxygen atom of S=O group or nitrogen atom of $-\text{NH}_2$ and imine $-\text{N}=\text{C}-$ groups, respectively²⁶. Upon complexation, there are some electronic changes due to the interaction of SZ ligand with calcium(II) and gold(III) metal ions. The UV-visible absorption spectrum of calcium(II) and gold(III) complexes have $\delta^1\delta^*$ transitions at 280 and 290 nm due to aromaticity of double bond characters²⁷. On the other side, the $n \rightarrow \pi^*$ transitions were recorded at the wavelengths 305 and 310 nm which can be assigned to amino, amido, and sulfonyl groups²⁸. The magnetic moments of Ca(II), Zn(II) and Au(III) complexes at room temperature have a diamagnetic character. The gold(III) complex also has a diamagnetic nature as expected for low spin d^8 complexes, which assigned to square planar geometry²⁹.

¹H-NMR spectra

The ¹H-NMR spectra of the SZ free ligand has the expected distinguish signals. ¹H-NMR chemical shifts of SZ drug are assigned in Scheme 1. The ¹H-NMR spectra of $[\text{Ca}(\text{SZ})(\text{Cl})_2] \cdot 8\text{H}_2\text{O}$ (**1**), $[\text{Zn}(\text{SZ})(\text{Cl})_2] \cdot 2\text{H}_2\text{O}$ (**2**) and $[\text{Au}(\text{SZ})(\text{Cl})_2] \cdot \text{Cl}$ (**3**)

complexes are shown in Fig. 5 and their chemical shifts are listed and assigned in Table 3. The CH_3 proton shows singlet at $\delta = 2.290$ ppm and isoxazole proton at $\delta = 6.107$ ppm. In addition a multiplet peak at $\delta = 6.598$ and 7.485 ppm may be due to aromatic protons and peak at $\delta = 10.95$ ppm is due to NH proton. The $-\text{NH}$ proton of sulfonylamid group in case of Ca(II) and Zn(II) complexes is disappears indicating the involvement of sulfonylamid nitrogen in the coordination, this result is contrary to the gold(III) complex, because of presence of $-\text{NH}$ proton. So, the sites of coordination are different from (Ca(II) and Zn(II)) and Au(III) complex. Signals observed in the calcium(II) and zinc(II) SZ complexes at region of $\delta = 3.368$ and 3.329 ppm, respectively are due to proton of uncoordinated water molecules.

Thermal analyses

TGA curves of the $[\text{Ca}(\text{SZ})(\text{Cl})_2] \cdot 8\text{H}_2\text{O}$ (**1**), $[\text{Zn}(\text{SZ})(\text{Cl})_2] \cdot 2\text{H}_2\text{O}$ (**2**) and $[\text{Au}(\text{SZ})(\text{Cl})_2] \cdot \text{Cl}$ (**3**) complexes are presented in Fig. 6. The first degradation step for calcium(II) and zinc(II) complexes occurs within temperature range of 30-200 °C due to the loss of uncoordinated water molecules. The second-to-third decomposition steps take place within the temperature range of 200-800 °C due to the loss of chlorine gas and decomposition of SZ molecule. The calcium(II) oxide CaO (Calc. 11.03%; Found 10.50%), zinc(II) oxide (Calc. 19.12%; Found 18.60%) and gold metal (Calc. 35.39%; Found 34.90%) are the final products remains stable till 800°C as final residues.

X-ray powder diffraction and SEM studies

Figure 7 shows the XRD patterns of the $[\text{Au}(\text{SZ})(\text{Cl})_2] \cdot \text{Cl}$ (**3**) complex. The main XRD peaks were observed in Fig. 7. The X-ray diffraction patterns confirms that the formed gold(III) complex is a crystalline behavior. The crystalline size diameter of the gold(III) nanoparticle has estimated using Deby-Scherrer formula [30] is 40 nm. The surface morphological and particle size discussions of the gold(III) nanoparticles were performed using scanning electron microscopy (SEM) and transmission electron microscopy (TEM) with pure images represented in Fig. 8. It is clearly obviously that the gold(III) complex is formed extremely fine as a leaf papers with aggregated structure.

Table 2: Distinguish Infrared spectral bands and their assignments of a free SZ ligand and their complexes

SZ	Ca(II)	Zn(II)	Au(III)	Assignments
3268	3464	3476	3585	$\nu(\text{NH})$; NH_2
3378		3386	3498	
3299	-	-	3383	$\nu(\text{NH})$; sulfonamido group
1623	1624	1621	1624	$\delta(\text{NH}_2)$
1597	1599	1596	1496	$\nu(\text{C}=\text{C})$; phenyl ring
1504	1503	1502		
1472	1471	1472	1469	Isoxazole ring
1439	1439	1438	1424	
1365	1364	1398		
1310	1309	1330	1322	$\nu_{\text{as}}(\text{SO}_2)$; sulfonyl group
1188	-	-	-	$\nu_{\text{s}}(\text{SO}_2)$; sulfonyl group
1152	1152	1161	1167	
-	548	548	511	$\nu(\text{M}-\text{O})$
-	400	429	441	$\nu(\text{M}-\text{N})$

Table 3: $^1\text{H-NMR}$ spectral data of free SZ drug and their Ca(II), Zn(II) and Au(III) complexes

Assignments	$\delta(\text{ppm})$			
	SZ	Ca(II)	Zn(II)	Au(III)
-NH	10.950	-	-	10.946
H; isoxazole	6.107	6.072	6.012	6.082
H; aromatic	6.598, 7.485	6.588, 7.459	6.572, 7.465	6.633, 7.490
H; NH_2	6.100	6.098	6.053	6.085
H; H_2O	-	3.368	3.329	-
H; CH_3	2.290	2.277	2.268	2.284

Table 4: The inhibitory activities against colon carcinoma and hepatocellular carcinoma cells for the $[\text{Au}(\text{SZ})(\text{Cl})_2]\cdot\text{Cl}$ (3) complex and doxorubicin drug

Sample conc. (μg)	Viability			
	HepG-2 cell line		HCT-116 cell line	
	doxorubicin	Au(III) complex	doxorubicin	Au(III) complex
50	4.91	16.72	6.82	30.92
25	8.87	36.28	8.89	46.73
12.5	14.83	48.25	14.83	68.08
6.25	16.16	73.56	16.16	81.45
3.125	25.28	85.94	22.28	91.32
1.56	34.64	94.16	34.64	96.47
0.78	45.79	98.78	45.78	98.96
0.39	51.08	100.00	51.28	100.00
0	100	100.00	100	100.00
IC_{50}	0.467 μg	2.77 μg	0.471 μg	3.41 μg

Antimicrobial assessments

In vitro cytotoxicity assessment of the $[\text{Au}(\text{SZ})(\text{Cl})_2]_2 \cdot \text{Cl}$ (**3**) complex was performed on human colon carcinoma (HCT-116) cell line and human hepatocellular carcinoma (HepG-2) cell line in the presence of doxorubicin standard drug. The results evaluated upon the determination of inhibitory concentration of 50 % (IC_{50}), the data was listed in Table 4. In comparison between data of $[\text{Au}(\text{SZ})(\text{Cl})_2]_2 \cdot \text{Cl}$ (**3**) complex and doxorubicin standard, the $[\text{Au}(\text{SZ})(\text{Cl})_2]_2 \cdot \text{Cl}$ (**3**) complex has IC_{50}

equal 21.10 and 23.1 μg for HepG-2 and HCT-116 cell line, respectively. From these data we can deduced that $[\text{Au}(\text{SZ})(\text{Cl})_2]_2 \cdot \text{Cl}$ (**3**) complex has an effective against HepG-2 cell line rather than HCT-116 cell line.

ACKNOWLEDGMENTS

This work was funded by Deanship of Scientific Research at university of Princess Nora Bint Abdul Rahman.

REFERENCES

- Moulton, B.; Zaworotko, M.J. *Chem. Rev.* **2001**, *101*, 1629.
- Wu, C.D.; Lu, C.Z.; Zhuang, H.H.; Huang, J.S. *J. Am. Chem. Soc.* **2002**, *124*, 3836.
- Dybtsev, D.N.; Chun, H.; Kim, K. *Angew. Chem. Int. Ed.* **2004**, *43*, 5033.
- Lpez-Gresa, M.P.; Ortiz, R.; Perell, L.; Latorre, J.; Liu-Gonzalez, M.; Garcya- Granda, S.; Perez-Priede, M.; Cantn, E. *J. Inorg. Biochem.* **2002**, *92*, 65.
- Yuan, R.X.; Xiong, R.G.; Abrahams, B.F.; Lee, G.H.; Peng, S.M.; Che, C.M.; You, X.Z. *J. Chem. Soc. Dalton Trans.* **2001**, 2071.
- Turel, I.; *Coord. Chem. Rev.* **2002**, *232*, 27.
- Xiao, D.R.; He, J.H.; Sun, D.Z.; Chen, H.Y.; Yan, S.W.; Wang, X.; Yang, J.; Yuan, R.; Wang, E.B. *Eur. J. Inorg. Chem.* **2012**, 1783.
- Drevensek, P.; Zupancic, T.; Pihlar, B.; Jerala, R.; Kolitsch, U.; Plaper, A.; Turel, I. *J. Inorg. Biochem.* **2005**, *99*, 432.
- Xiao, D.R.; Wang, E.B.; An, H.Y.; Su, Z.M.; Li, Y.G.; Gao, L.; Sun, C.Y.; Xu, L. *Chem. Eur. J.* **2005**, *11*, 6673.
- He, J.H.; Xiao, D.R.; Chen, H.Y.; Yan, S.W.; Sun, D.Z.; Wang, X.; Yang, J.; Yuan, R.; Wang, E.B. *Inorg. Chim. Acta.* **2012**, *385*, 170.
- Kathawate, L.; Sproules, S.; Pawar, O.; Markad, G.; Haram, S.; Puranik, V.; Salunke-Gawali, S. *J. Mol. Struct.* **2013**, *1048*, 223.
- Beerlev, W.N.; Pelers, W.; Mager, K.; *Ann. Trop. Med. Parasite.* **1960**, *26*, 288.
- Hoffman La Roche Co., Swiss Patent No. 416648, **1967**.
- Sharaby, C.; *Synth. React. Inorg. Met. Org. Chem.* **2005**, *35*, 133.
- Garg, S.K.; Ghosh, S.S.; Mathur, V.S. *Int. J. Clin. Pharm. Therapy. Toxicol.* **1986**, *24(1)*, 23.
- Ferrer, S.; Borrás, J.; Garcia-Esparia, E. *J. Inorg. Biochem.* **1990**, *39*, 297.
- Supuran, C.T.; Minicione, F.; Scozzafav, A.; Briganti, F.; Minicinone, G.; Ilises, M.A. *Eur. J. Med. Chem.* **1998**, *33*, 247.
- Blasco, F.; Perello, L.; Latorre, J.; Borra, J.; Garcia-Granda, S.J. *Inorg. Biochem.* **1996**, *61*, 143.
- Blasco, F.; Ortiz, R.; Perello, L.; Borrás, J.; Amigo, J.; Debaerdemaeker, T. *J. Inorg. Biochem.* **1994**, *53*, 117.
- Bellú, S.; Hure, E.; Trapé, M.; Rizzotto, M.; Sutich, E.; Sigrist, M.; Moreno, V. *Quim. Nova.* **2003**, *26(2)*, 188.
- Mosmann, T. *J. Immunol. Methods.* **1983**, *55*, 65.
- Gangadevi, V.; Muthumary, J. *African J. Biotechnology.* **2007**, *6*, 1382.
- Geary, W.J. *Coord. Chem. Rev.* **1971**, *7*, 81.
- Nakamoto, K. "Infrared and Raman spectra of inorganic and coordination compound". New York: Wiley, **1978**.
- Melina, M.; Fernando P.; de Souza, P.C.; Leite, C.Q.; Javier E.; Nascimento, O.R.; Gianella F.; Torre, M.H. *J. Mol. Str.* **2013**, *1036*, 180.
- Chohan, Z.H.; Shad, H.A.; Nasim F.H. *Appl. Organometal. Chem.* **2009**, *23(8)*, 319.
- Ozturk, O.F.; Sekerci, M.; Ozdemir, E. *Russ. J. Coord. Chem.* **2005**, *31*, 687.
- Ozturk, O.F.; Sekerci, M.; Ozdemir, E. *Russ J Gen Chem.* **2006**, *76*, 33.
- Abdalrazaq, E.A.; Buttrus, N.H.; Abd Al-Rahman, A.A. *Asian J. Chem.* **2010**, *22(3)*, 2179.
- Cullity, B.D. "Elements of X-ray Diffraction", Addison-Wesley, Reading, MA, **1972**, 102.